POLİTEKNİK DERGİSİ

JOURNAL of POLYTECHNIC

ISSN: 1302-0900 (PRINT), ISSN: 2147-9429 (ONLINE)
URL: http://dergipark.org.tr/politeknik

Development of a high-efficiency double air gap axial flux synchronous reluctance motor for electric vehicles: Effect of magnet assistance

Elektrikli araçlar için yüksek verimli çift hava aralıklı eksenel akılı senkron relüktans motorun geliştirilmesi: Mıknatıs desteğinin etkisi

***Yazar(lar) (Author(s))**: Emre GÖZÜAÇIK[1], Mehmet AKAR[2]*

ORCID[1]: 0000-0003-2807-8187

ORCID[2]: 0000-0003-0164-1451

To cite to this article: Gözüaçık E., and Akar M., "Development of a High-Efficiency Double Air Gap Axial Flux Synchronous Reluctance Motor for Electric Vehicles: Effect of Magnet Assistance", ***Journal of Polytechnic***, 29(4):290435:1-11 (2026).

Bu makaleye şu şekilde atıfta bulunabilirsiniz: Gözüaçık E. ve Akar M., "Development of a High-Efficiency Double Air Gap Axial Flux Synchronous Reluctance Motor for Electric Vehicles: Effect of Magnet Assistance", ***Politeknik Dergisi***, 29(4):290435:1-11 (2026).

Erişim linki (To link to this article): http://dergipark.org.tr/politeknik/archive

DOI: 10.2339/politeknik.1761080

Development of a High-Efficiency Double Air Gap Axial Flux Synchronous Reluctance Motor for Electric Vehicles: Effect of Magnet Assistance

Highlights

- *An axial flux synchronous reluctance motor (AF-SynRM) was designed and analyzed for electric vehicle applications with a focus on high efficiency*
- *Different pole numbers (6, 8, and 10) and double air-gap topologies (double stator and double rotor) were compared at 30 kW rated power.*
- *Ferrite and rare-earth magnets were introduced into the magnet-free model to assess the effect of assisted magnets on efficiency and power density.*
- *The study provides design insights for improving efficiency in AF-SynRMs and contributes to early-stage development strategies for axial flux EV motors.*

Graphical Abstract

Graphical abstract illustrates the impact of pole number, double air-gap topologies, and magnet-assistance on the efficiency of axial flux synchronous reluctance motors.

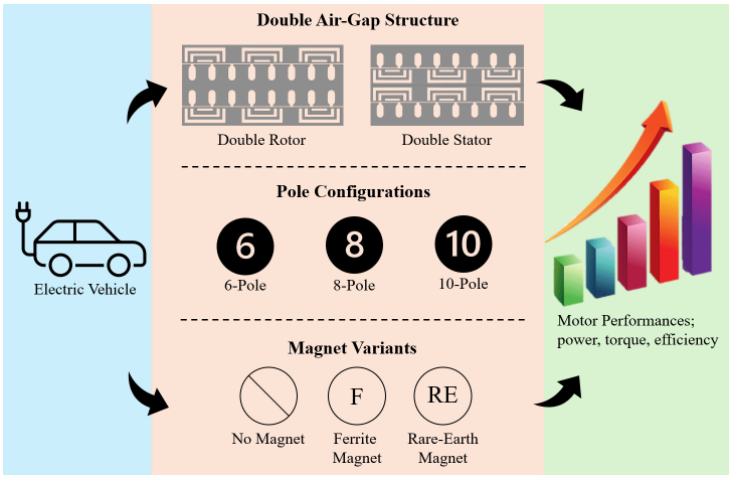

Figure. Graphical Abstract

Aim

This study aims to design a high-efficiency axial flux synchronous reluctance motor (AF-SynRM) for electric vehicle applications and to comparatively analyze its performance parameters.

Design & Methodology

This study models 30 kW AF-SynRM topologies with 6, 8, and 10 poles in double air-gap configurations, evaluating magnet-free, ferrite, and rare-earth magnet designs for improved power density.

Originality

This study systematically compares pole number, double air-gap topologies, and magnetic assistance in axial flux motors to provide a comprehensive efficiency assessment and address a literature gap.

Findings

Pole number and magnetic assistance strongly affect motor efficiency, with rare-earth magnets notably improving performance in limited volume designs.

Conclusion

The study offers findings that can guide early-stage axial flux motor designs and contributes to the development of high-efficiency electric vehicle motors.

Declaration of Ethical Standards

The author(s) of this article declare that the materials and methods used in this study do not require ethical committee permission and/or legal-special permission.

Development of a High-Efficiency Double Air Gap Axial Flux Synchronous Reluctance Motor for Electric Vehicles: Effect of Magnet Assistance

Araştırma Makalesi / Research Article

Emre GÖZÜAÇIK[1*], Mehmet AKAR[1]

[1]Faculty of Engineering and Architecture, Electrical and Electronics Engineering Department, Tokat Gaziosmanpaşa University, 60250 Tokat, Türkiye

(Geliş/Received : 09.08.2025 ; Kabul/Accepted : 26.12.2025 ; Erken Görünüm/Early View : 05.01.2026)

ABSTRACT

This study develops the Axial Flux Synchronous Reluctance Motor (AF-SynRM) design with low volume, low loss and high efficiency has been preferred for use in EV. Double air-gap AF-SynRM 2D linear models with different pole numbers (6, 8, and 10) were tested using the Finite Element Method (FEM). The magnet condition was considered (magnet-free, ferrite magnet-assisted, rare-earth magnet-assisted). The models were compared in terms of torque, power, and efficiency. This study aims to address the lack of 2D linear models and reduce the computational intensity in the design process. The 10-pole magnet-assisted AF-SynRM model exhibits a torque/ampere ratio of 1.87, a power density of 4.8 kW/kg and efficiency of 92.75%. This study used 18 different AF-SynRM models in the initial design process, ensuring the optimal model emerges in terms of high torque, power, and efficiency.

Keywords: Electric vehicles (EV), double air gap axial flux motors, synchronous reluctance motors (SynRM), ferrite magnet assisted motors, rare earth magnet assisted motors.

Elektrikli Araçlar için Yüksek Verimli Çift Hava Aralıklı Eksenel Akılı Senkron Relüktans Motorun Geliştirilmesi: Mıknatıs Desteğinin Etkisi

ÖZ

Bu çalışma, düşük hacim, düşük kayıp ve yüksek verimlilik özelliklerine sahip ve elektrikli araçlar için Eksenel Akılı Senkron Relüktans Motoru (EA-SRM) tasarımını geliştirmektedir. Çift hava aralıklı (çift rotor ve çift stator), farklı kutup sayısına sahip (6-8-10 kutup) EA-SRM 2D lineer modelleri mıknatıs durumuna (Mıknatıssız, ferrit mıknatıs destekli ve nadir toprak elementi mıknatıs destekli) göre Sonlu Elemanlar Yöntemi (SEY) kullanılarak test edilmiştir. EA-SRM modeli için hava aralığı topolojisi, kutup sayısı ve mıknatıs etkisi tork, güç ve verimlilik açısından kıyaslanmıştır. Bu çalışmada çift hava aralıklı EA-SRM tasarımının literatürdeki eksikliğinin giderilmesi ve 2D lineer modeller kullanarak tasarım sürecindeki işlem yoğunluğunu minimuma indirmek amaçlanmıştır. 10 kutuplu mıknatıs destekli EA-SRM modeli, 1.87 Nm/A tork/akım oranı, 4.8 kW/kg güç yoğunluğu ve %92.75 verimlilik sergilemektedir. Bu çalışma sayesinde EA-SRM'ye ait 18 farklı model ilk tasarım sürecine katkıda bulunmuştur. Yüksek tork, güç ve verim açısından optimum modelin ortaya çıkarılmasını sağlamaktadır.

Anahtar Kelimeler: Elektrikli Araçlar (EA), çift hava aralıklı eksenel akılı motorlar, senkron relüktans motorlar (SRM), ferrit mıknatıs destekli motorlar, nadir toprak elementi mıknatıs destekli motorlar.

1. INTRODUCTION

Today, the emission of greenhouse gases leads to many disasters such as air pollution, climate change and global warming. Worldwide, 14% of the emissions of greenhouse gases such as CO_2, NO, CO and methane come from the transport industry due to fossil fuel vehicles [1]. Although efforts are being made to switch to renewable energy sources for industrial use and to reduce emissions from internal combustion vehicles, population growth, urbanization and increased vehicle use require other solution. In this case, EV appear to be the best alternative. Although they currently have a small market volume, they are expected to dominate the market in the coming years [1].

Electric motors for use in EV are expected to have high torque at low speeds for acceleration or hill-climbing, high power at high speeds for cruising/highway driving, and a wide Constant Power Speed Range (CPSR) [2], [3]. Basic performance parameters such as high-power density, high torque density, wide speed range, efficiency, cost and reliability are important in motor selection. In addition, parameters such as fault tolerance, durability, thermal tolerance, torque ripple and acoustic noise are also critical to motor performance [2], [4], [5], [6], [7].

*Sorumlu Yazar (Corresponding Author)
e-posta : emre.gozuacik@gop.edu.tr

In terms of motor topology, there are radial flux motors with the flux direction perpendicular to the motor rotation axis and Axial Flux (AF) motors with the flux direction parallel to the shaft axis [8], [9]. AF motors are disadvantaged compared to radial motors because of the motor discs from the large axial force between the stator and rotor, the difficulty of manufacturing laminated cores, the costly and difficult assembly process. They have a shorter axial length compared to the outer diameter (hence smaller volume), high torque density due to the increase in air gap area within the same volume, a compact geometric shape and a superior power to weight ratio. It is also preferred in EV applications due to its volumetric advantage, axial structure, and high performance [4], [9], [10], [11].

AF motors are analysed in different topologies according to the number of air gaps and the cycle of the flux path. Double air gaps are used as Double Rotor (DR) or Double Stator (DS). In addition, a multi-sided design with increased air gap has been added to the literature. In cases where the motor diameter is limited, multiple air gap structures are preferred for high power and torque density [4], [11], [12].

Electric motors, which are one of the important parts of EV, continue to be studied under different topologies depending on their basic characteristics, control methods and performance values [13]. SynRM has a motor topology that can be used in EV as a traction motor against strong competitors such as IM and PMSM. SynRMs are robust and fault tolerant like IMs, efficient like PM motors, have a small structure and similar control methods. In addition, unlike IM and PMs, there are no windings, bars or magnets in the rotor, avoiding negative effects such as increased losses and demagnetization [5], [14]. SynRMs, which have lower ripple and higher efficiency compared to switched reluctance motors with similar structure, also operate more quietly [15]. SynRMs can generate reluctance torque due to their anisotropic rotor structure. It also has the advantages of simple and durable structure, low cost, high torque and field weakening capability [5], [16]. The main problems with these motors are known to be control issues, manufacturing difficulties, high torque ripple and low power factor [2], [5], [14]. Rotor structures are effective on ripple, different barrier geometries reduce torque harmonics, and power factor increases with increasing saliency ratio [5], [7]. As a result, SynRMs have disadvantages that can be reduced by variable rotor structure and optimization methods.

If magnets are added to the barrier structure, the SynRMs are called Permanent Magnet-assisted SynRM (PMa-SynRM). There are improvements in power factor, torque, efficiency, and saliency ratio compared to SynRMs. PMa-SynRMs are gaining importance in the automotive industry along with IPMs with similar structure. Compared to IPMs, PMa-SynRMs maintain their advantage due to the fact that they use a smaller volume of magnets, have a wider speed range in the constant power region and have a higher saliency ratio [6], [7], [13], [17], [18]. The pole-slot combination, barrier structure and number are optimised to obtain the ideal design [19]. In addition, differences in the shape and position of the inserted magnets in the flux barriers make important contributions to the performance of these motors.

Ferrite magnets are cheaper and easier to supply than rare-earth (RE) magnets but are more disadvantageous in terms of flux density and coercivity. Problems such as decreasing magnetic torque compared to RE magnet motors can be solved by increasing the number or volume of ferrite magnets [20]. For SynRM, the ferrite-assisted motor becomes advantageous in terms of performance data such as torque, efficiency and power factor compared to a magnet-free motor [21]. Furthermore, the torque capacity and field weakening capability of the SynRM can be enhanced by incorporating a ferrite magnet, particularly in applications where high CPSR is required. This makes it a viable alternative to RE magnet competitors such as IPM in EV applications [22].

The study in Gerçekcioğlu and Akar (2021) optimized the "U" barrier structure of the AF-SynRM model with a single air gap, achieving power values of 2.2 kW, torque values of 13.93 Nm, and efficiency values of 89.3% at full load [23]. To contribute to similar studies in the literature, different configurations of the AF-SynRM model with a "U" barrier structure were developed to reach a power value of 30 kW, depending on the air gap topology, pole number, and magnet effect parameters. To determine the optimal model among the 18 developed, 2D analyses were simulated using FEM, which provided faster results with accuracy similar to that of 3D analysis. Notably, linear analyses of AF-SynRM models with double air gaps are anticipated to make significant scientific contributions to the field.

In this study, the initial designs of double-sided AF-SynRM were compared in detail, with the aim of identifying the most efficient design. The AF-SynRM is studied at different pole numbers (6-8-10 poles). As a main contribution, the effect of magnet-free and magnet-assisted models on the design of an AF-SynRM for EV is clearly demonstrated. These models are compared according to the results of power, torque and efficiency analyses. In order to select the most efficient model, the points to consider for the initial design and the differences between models are highlighted.

2. MATERIAL and METHOD

In the design of an electric vehicle motor, it is essential to consider several factors, including the mechanical design parameters of the vehicle, the environmental conditions and the intended use. The vehicle weight, tyre diameter, mechanical transmission elements, road condition, traffic and speed capacity, driving test standards and performance expectations are used to determine the force and power value that the vehicle's motor should provide [24]. The required and expected motor parameters are determined by traction force/power

calculations for motor topology selection and EV. The initial motor parameters are given in Table 1.

Table 1. Motor Initial Parameters

Description	Value
Power (W)	30000
DC Bus Voltage (V)	600
Efficiency (%)	>90
Maximum Speed (rpm)	10000
Rated Speed (rpm)	3000
Stator Connection Type	Star
Number of Phase	3

SynRMs have a similar stator structure to IM. In this case, the stator design involves the same steps as the IM stator design [25], [26]. AF-SynRM stator design calculations are used to determine design parameters such as stator outer diameter, stator inner diameter, number of slots, number of windings [24].

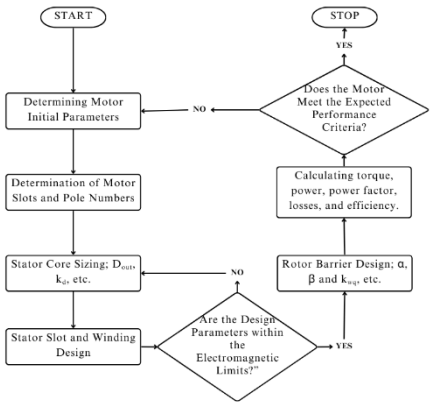

Figure 1. Flowchart of AF-SynRM Initial Design

Figure 1 shows the procedure diagram of the mathematical calculations for the initial design of the AF-SynRM. The process of designing the stator and rotor begins with the definition of initial parameters and ends with the detailed design. The design is finalized when the performance parameters, such as torque, power, power factor, losses, and efficiency, meet the expected criteria. AF-SynRM has a geometrically tapered structure from the outer diameter to the inner diameter. In this case, the tooth width varies in the inner and outer diameters. For this reason, the ratio of the stator inner diameter to the outer diameter k_D, given in Equation 1, is an important factor when designing the stator [24]. The motor outer diameter dimension is directly related to the power and performance of the motor with the standard coefficient in radial ($\propto D^2L$) and AF ($\propto D^3$) motors [24], [25].

$$k_D = \frac{1}{8}(1+k_d)(1-k_d^2) \tag{1}$$

$$D_{out} = \sqrt[3]{\frac{\in .P_{out}}{\pi^2 .k_D .k_{w1} .n_s .B_{mg} .A_m .\eta .\cos\phi}} \tag{2}$$

The formula for the AF-SynRM stator outer diameter is given in Equation 2. In this formula, $\in$ is the ratio of the back EMF to the phase voltage in the windings, P_{out} the output power, k_{w1} the winding factor, n_s the number of windings, B_{mg} the maximum flux density of the air gap, A_m the ampere per meter, η the efficiency, $\cos\phi$ the power factor [24].

Since SynRM will generate a reluctance torque due to its anisotropic structure, the number, shape, and placement of the barriers are important factors in the rotor design. In their study, Gerçekcioğlu and Akar (2021) observed an improvement in torque with an increase in the number of barriers, in particular a large reduction in torque ripple and an increase in power factor [23].

$$T_{em} = \frac{3}{2}p(L_d - L_q)i_d i_q = \frac{3}{2}p(L_d - L_q)I_m \sin(2\gamma) \tag{3}$$

$$pf = (L_d/L_q - 1)\sqrt{\frac{\sin(\pi - 2\gamma)}{\tan(\pi/2 - \gamma) + (L_d/L_q)^2 \cot(\pi/2 - \gamma)}} \tag{4}$$

In Equation 3, p is the pole pair, L_d, L_q are the inductance in the d and q axis, i_d and i_q are the stator current in the d and q axis, I_m is the stator current amplitude and γ is the current angle. The torque T_{em} produced in the motor is given by Equation 3 and the power factor pf formula is given by Equation 4 [23]. These values, which depend on the inductance values in the d and q axis of the motor, are directly related to the anisotropic structure of the rotor and therefore to the barrier structure, number, and placement [10], [23], [27].

$$P_{CoreLoss} = \sum_{n=1}^{N}(K_h(nf)B_n^2 + K_c(nfB_n)^2 + K_e(nfB_n)^{1.5}) \tag{5}$$

Total core losses are calculated using Equation 5, which is based on the non-constant parameters K_h, K_c and K_e. Equation 5 also gives the harmonic number n, the magnetic flux density B_n and the frequency f. The hysteresis, eddy and excess loss coefficients depend on the sheet material used in the stator and rotor. In magnet assisted motors, eddy currents are generated depending on the magnet's conductivity; these currents are proportional to the magnet's volume [28].

$$\eta = \frac{P_{out}}{P_{out} + P_{Tloss}}$$
$$TotalLoss = CoreLoss + SolidLoss + ... \tag{6}$$
$$... + StrandedLoss + MechanicalLoss$$

The AF-SynRM efficiency calculation is performed using Equation 6. In this equation, η is represented by efficiency, P_{out} by output power, and P_{Tloss} by total loss. In the AF-SynRM 2D linear model, total losses were obtained using the Ansys Maxwell Electrical Machine Design Toolkit. This toolkit can analyze motor efficiency, torque and other performance parameters, and these have been industrially verified. Total losses were included in Equation 6 as core loss, solid loss, stranded loss, and mechanical loss [28]. Roshandle et al. (2021) noted in their study that mechanical losses in motors designed for EVs above the nominal speed are between 0.5% and 3% of the nominal power [29].

When determining the number of rotor barriers, the rotor barrier angle α and the control angle of the alpha angle appear as β variables. In Equation 7, n_{layer} is the number of barriers. This equation gives the relationship between the α and β angles. It has been observed that the α angle reduces the torque ripple and the α/β ratio can vary in the studies [30].

$$\alpha = \frac{\pi/2p - \beta}{n_{layer} + 1/2} \tag{7}$$

It is used to find the barrier and segment widths by determining the control angles in rotor design. The ratio of barrier width (l_b) to segment width (l_s) is expressed as insulation ratio $k_{wq} = l_b/l_s$. Barrier and segment widths are calculated depending on the magnetomotive force distribution on the rotor d and q axis. Aghazadeh et al. (2019) investigated the effect of varying the insulation ratio between 0.2-1.2 on the average torque [27].

3. DESIGN AND ANALYSIS OF DOUBLE AIR GAP AF-SYNRM

In this study, a double air gap AF-SynRM has been designed. The design is realized with a rotor with a U-shaped barrier structure, an example of which can be found in the literature [23]. Due to the volumetric advantage of AF motors over their radial counterparts, they have higher torque and power density and less axial length [11]. For these reasons, the AF motor is preferred in this study. Depending on the number of air gaps of the AF motor topology, it is classified as DS, DR or multi air gap. The double air gap AF topology was preferred in this study as it provides an advantage in the average torque value and eliminates the negative effects of magnetic attraction between the rotor and stator [24], [31], [32].

The AF-SynRM DS and DR models are shown in Figure 2. In the models, the stator, rotor, and coils are given as 1-2-3 respectively. Despite the beneficial impact of the number of barriers in the SynRM, particularly to reduce torque ripple, the number of barriers is constrained to three in order to prevent an increase in the axial length.

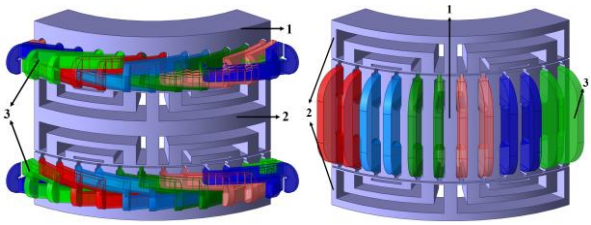

(a) (b)

Figure 2. Double Air Gap 3D Motor ¼ Model (1-Stator, 2-Rotor, 3-Coils); a) AF-DS-SynRM b) AF-DR-SynRM

Once the requirements and expectations for the motor design had been established, the rotor design k_{wq} and the α/β ratio were determined. In the preliminary design studies, the insulation ratio $k_{wq} = 1$ and the barrier/control angle ratio $\beta = 0.5\alpha$ were used [33].

In the AF-SynRM motor design, a distributed winding with a winding factor of 0.95 and a fill factor of 65-70% is preferred. Distributed windings provide higher reluctance torque than concentrated windings [23]. Walker et al. (2016) compared distributed and concentrated windings in their study. In this study, although the distributed winding design requires slightly higher current, similar torque values at maximum speed were achieved with the concentrated winding design [34]. Concentrated windings have advantages such as shorter winding ends, lower copper losses, ease of manufacture and high-power density. However, there are no significant differences in this area compared to the distributed winding. Distributed windings are becoming more popular for traction motors due to their higher efficiency at high speeds, lower cost, high fill factor and non-sinusoidal voltage induction of concentrated windings [34].

As stated in the literature, motor models with different numbers of poles and slots were created for the optimal SynRM model design. According to the results of the sizing analyses, the motor design parameters shown in Table 2 were obtained [33].

Table 2. Motor Design Parameters [33]

Description	6 Poles	8 Poles	10 Poles
Stator/Rotor Outer Diameter (mm)	203	210	242
Stator/Rotor Inner Diameter (mm)	142	150	181.5
Number of Stator Slots	36	48	60
Stator Axial Length (Single Stator) (mm)	35	35	35
Air gap (mm)	1	1	1
Material of Stator and Rotor	JFE Steel_35JN250		

In this study, the parameters given in Table 2 are modelled for a 3-barrier AF-SynRM design. These parameters were added to the ANSYS software, which can perform FEM motor analysis, and models were generated. For the DS and DR structures, changes were made to the winding structure and added to the ANSYS

software. Although the magnetic attraction effect between the rotor and stator is neutralized in the double air gap AF motor designs, the air gap is assumed to be 1 mm due to manufacturing issues [33].

3.1. AF-SynRM 2D Linear Motor Design

The analysis software used for motor design can perform 2D or 3D analysis with FEM. In the studies, the results obtained by these analysis software with the 3D FEM model have been confirmed by experimental studies [35]. Although 3D analysis results are precise and accurate, they have a high number of meshes and therefore require a long processing time. In this case, researchers prefer 2D analyses with fewer mesh numbers, which give fast results with acceptable accuracy [36]. A study by Gulec and Aydin (2018) reported that 2D linear models require approximately 20 times less mesh than 3D models and complete analyses 114 times faster. However, the difference in torque results was only 1.3% [37].

While radial machines are suitable for 2D analysis due to their axisymmetric structure, AF motors require 3D analysis due to their 3D flux path and non-axisymmetric structure. AF motors can be modelled as a linear model to take advantage of 2D analysis. For 2D linear analysis of AF, a moment arm is created by averaging the outer and inner circumferential lengths of the motor and linear motion is assumed instead of circular motion. It has been observed in the literature that 2D AF motor analysis provides similar results to 3D analysis in a much shorter time [38]. Especially in the initial design and modelling phase, it provides many models and analysis possibilities in a short time.

In this study, double air gap 2D model designs of the motors, whose parameters are given in Table 2, were carried out. Due to the double air gap topology, two different designs were realized for each motor as DR and DS. These designs were analyzed using a current source in 2D linear analysis.

$$
\begin{aligned}
I_{phase(a)} &= I_{\max}.\sin(n.\frac{2p}{60}.\pi.t+\gamma-\square) \\
I_{phase(b)} &= I_{\max}.\sin(n.\frac{2p}{60}.\pi.t+\gamma-\frac{2\pi}{3}-\square) \\
I_{phase(c)} &= I_{\max}.\sin(n.\frac{2p}{60}.\pi.t+\gamma-\frac{4\pi}{3}-\square)
\end{aligned} \tag{8}
$$

Three phase current formulas ($I_{phase(a)}, I_{phase(b)}, I_{phase(c)}$) for the current source are given in Equation 8. In this equation, n represents the revolutions per minute (rpm), p pole pair, t time, γ current angle and $\square$ initial angle [23], [39]. For the first models, parametric analysis was performed over the current angle (γ) to find the Maximum Torque per Ampere (MTPA) point. The remaining analyses were performed as a function of the MTPA current angle at which the maximum torque was obtained.

3.2. Comparison of AF-SynRM Magnet-Assisted Models

In order for AF-SynRM to achieve higher torque and power density, magnets have been added to the design barriers [18]. The aim of the study is to improve motor performance using Y30 - Ferrite Magnet (0.4T). This avoids the disadvantages of RE magnets such as cost and supply constraints. In order to compare the contribution of ferrite magnets to motor performance, RE N42SH - Neodymium Iron Boron (NdFeB) magnets (1.451T) assisted motor analyses were also carried out.

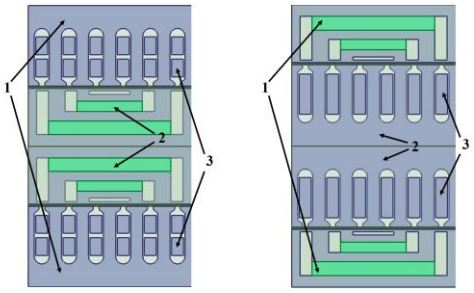

(a) (b)

Figure 3. Double Air Gap 2D Linear Motor Model (1-Stator, 2-Magnets, 3-Coils); a) AF-DS-PMa-SynRM b) AF-DR-PMa-SynRM

The 2D linear models of the AF double air gap magnet-assisted SynRM (AF-DS-PMa-SynRM / AF-DR-PMa-SynRM) are shown in Figure 3a and Figure 3b. In the models, the stators, magnets, and coils are given as 1-2-3 respectively. The magnets have been added to fit into the horizontal spaces of the wide barriers. This increases the resistance to axial forces acting on the barriers.

The results of the DR and DS models obtained from the analyses are presented in Table 3 according to the minimum current density . The DR and DS topologies of the AF-SynRM and AF-PMa-SynRM (Y-30 (Ferrite) and N42SH (RE) assisted) models are compared as 6, 8 and 10 pole designs depending on the current density. For motors that require high power in a low volume, such as EV, cooling is required due to high current operation [33]. Stator current density also varies with different cooling methods [40]. The choice of stator cooling jacket and direct forced liquid cooling allows current densities between 10 A/mm^2 and 30 A/mm^2 in the design. The study by Gai et al. (2019) presents performance data for EVs on the market that use a stator cooling jacket system [41]. Analyses were conducted to investigate the effects of numbers of poles, various motor volume, and different magnet type (magnet-free, ferrite, RE) values within the range of current density values.

Table 3. Comparison of AF-SynRM Models at 10 A/mm^2 Current Density

	Current Density (*J*)	**10 (A/mm^2)**								
	Description	**AF-SynRM**			**AF-PMa-SynRM (Y-30)**			**AF-PMa-SynRM (N42SH)**		
AF-DS-SynRM	Pole Numbers	6	8	10	6	8	10	6	8	10
	MTPA Current Angle (γ)	44	42	42	37	37	36	9	11	14
	Torque (Nm)	24.68	35.23	52.58	32.46	50.14	77.48	40.77	61.15	94.04
	Torque/Ampere (Nm/A)	0.77	0.80	0.83	1.03	1.16	1.23	1.14	1.34	1.45
	Power (kW)	7.75	11.06	16.51	10.2	15.75	24.34	12.81	19.21	29.54
	Power Density (kW/kg)	0.54	0.78	1.02	0.59	0.93	1.28	0.74	1.13	1.55
	Efficiency (%)	85.5	87.71	88.07	89	91.39	91.85	88.93	92.12	92.75
	Stator Winding Resistance (Ω)	0.342	0.203	0.139	0.342	0.203	0.139	0.342	0.203	0.139
	Description	**AF-SynRM**			**AF-PMa-SynRM (Y-30)**			**AF-PMa-SynRM (N42SH)**		
AF-DR-SynRM	Pole Numbers	6	8	10	6	8	10	6	8	10
	MTPA Current Angle (γ)	31	28	28	25	23	23	2	3	4
	Torque (Nm)	29.7	43.38	61.71	41.05	62.95	92.45	47.55	79.97	120.53
	Torque/Ampere (Nm/A)	0.82	0.82	0.83	1.13	1.19	1.24	1.21	1.36	1.46
	Power (kW)	9.33	13.63	19.39	12.9	19.77	29.04	14.94	25.12	37.8
	Power Density (kW/kg)	0.67	0.93	1.12	0.77	1.13	1.44	0.90	1.44	1.88
	Efficiency (%)	83.91	86.79	87.41	87.65	90.47	91.14	87.88	90.95	91.91
	Stator Winding Resistance (Ω)	0.377	0.198	0.132	0.377	0.198	0.132	0.377	0.198	0.132

Table 3 shows the analysis results for the AF-SynRM models comparison at 10 A/mm^2 current density and 3000 rpm rated speed. In the analyses, the MTPA current angles, which vary according to the DR-DS topology, the number of poles and the state of the magnet, were calculated according to the maximum torque. As the number of poles and the motor volume increase, the performance of the models improves. The best output power was obtained with the 10-pole RE assisted AF-DR-SynRM model. In this model, the motor achieved a power of 37.8 kW, a torque of 120.53 Nm and an efficiency value of 91.91%. The maximum power for the 6-pole and 8-pole RE assisted AF-DR-SynRM models are analysed as 14.94 kW, 25.12 kW respectively. In this case it was observed that the 6 and 8 pole models could not reach the rated power of 30 kW. As illustrated in Table 3, the AF-DR-SynRM models demonstrate higher power and torque output than the AF-DS-SynRM models. The 10-pole RE assisted AF-DS-SynRM model achieves 29.54 kW, close to the rated power with maximum efficiency of 92.75%. It achieves notable results in terms of minimum current density.

The ferrite-assisted AF-DR-SynRM models approach, but do not reach, the 30 kW rated power performance criterion as the number of poles increases. At a current density of 10 A/mm^2, 6-8-10 pole ferrite-assisted motors achieved 12.9 kW, 19.77 kW and 29.04 kW respectively. None of the 6 and 8 pole models could achieve a rated power of 30 kW at minimum current density. The best magnet-free model was the 10-pole DR-AF-SynRM with 19.39 kW power, 61.71 Nm torque and 87.41% efficiency.

In these analyses, which are performed at a constant speed of 3000 rpm, power, and torque change in direct proportion to each other. The resistance of the stator winding depends on the number of coils and the diameter of the coil. Since winding resistance has a direct effect on copper loss, it has a negative impact on efficiency. In the 10-pole model, one of the reasons for the high efficiency is the low winding resistance. Torque is directly proportional to current as shown in Equation 3. The torque/ampere is given to indicate the effect of a change in current on torque. In Table 3, the RE-assisted AF-DR-SynRM 10-pole model achieved the highest torque/ampere ratio 1.46 Nm/A and power density 1.88 kW/kg at 10 A/mm^2. In order to improve the inadequate performance values, all AF-SynRM models are analysed at higher current (30 A/mm^2 current density) in the following sections.

Table 4 compares the peak power values of all AF-SynRM models at 30 A/mm^2 current density. In Table 3, results at different MTPA current angles were derived from the analyses performed at 10 A/mm^2 current density. The highest power value of 96.74 kW was achieved for the RE-assisted AF-DR-SynRM model. For this model, torque values of 307.94 Nm and efficiency values of 81.26% were obtained. When evaluated at 30 kW rated power, the 6-pole ferrite-assisted models as well as the 6-8 pole magnet-free models are not sufficient despite the high current density. Compared to the low current analyses, the peak current efficiencies decreased. Due to the positive effect of the number of poles on the motor performance, the maximum power of the 10-pole magnet-free, ferrite-assisted and RE-assisted AF-DR-SynRM models is 41.43 kW, 64.99 kW and 96.4 kW respectively. The 10-pole model has a maximum power density of 4.8 kW/kg. As with the low current density, the maximum efficiency of the RE-assisted AF-DS-SynRM model is 83.79%. Although the increase in current leads to an increase in torque in the models analyzed, the torque/ampere ratio decreases according to Table 4. The maximum torque/ampere ratio is 1.44 Nm/A for the 10-pole RE-assisted AF-DS-SynRM model.

Table 4. Comparison of AF-SynRM Models at 30 A/mm^2 Current Density

	Current Density (*J*)	**30 (A/mm^2)**								
	Description	**AF-SynRM**			**AF-PMa-SynRM (Y-30)**			**AF-PMa-SynRM (N42SH)**		
AF-DS-SynRM	Pole Numbers	6	8	10	6	8	10	6	8	10
	MTPA Current Angle (γ)	44	44	42	36	35	33	33	35	36
	Torque (Nm)	59.33	86.61	123.78	79.76	114.34	166.59	109.35	175.74	270.47
	Torque/Ampere (Nm/A)	0.62	0.65	0.65	0.85	0.88	0.89	1.17	1.35	1.44
	Power (kW)	18.64	27.21	38.89	25.06	35.92	52.34	34.35	55.21	84.97
	Power Density (kW/kg)	1.29	1.92	2.40	1.46	2.11	2.75	2.00	3.25	4.47
	Efficiency (%)	63.8	69.54	69.84	71.48	75.8	76.37	76.65	82.77	83.79
	Stator Winding Resistance (Ω)	0.342	0.203	0.139	0.342	0.203	0.139	0.342	0.203	0.139
	Description	**AF-SynRM**			**AF-PMa-SynRM (Y-30)**			**AF-PMa-SynRM (N42SH)**		
AF-DR-SynRM	Pole Numbers	6	8	10	6	8	10	6	8	10
	MTPA Current Angle (γ)	26	27	27	19	18	23	19	20	21
	Torque (Nm)	66.27	97.34	136.49	87.93	128.83	176.43	131.87	206.86	307.94
	Torque/Ampere (Nm/A)	0.61	0.62	0.61	0.80	0.80	0.79	1.20	1.29	1.37
	Power (kW)	20.82	30.58	42.88	27.62	39.53	55.43	41.43	64.99	96.74
	Power Density (kW/kg)	1.50	2.08	2.47	1.66	2.26	2.75	2.49	3.72	4.80
	Efficiency (%)	58.8	65.58	66.61	65.09	70.23	71.75	72.12	79.47	81.26
	Stator Winding Resistance (Ω)	0.377	0.198	0.132	0.377	0.198	0.132	0.377	0.198	0.132

For the magnet-assisted (ferrite and RE) AF-DR-SynRM and AF-DS-SynRM, the 8-pole and 10-pole models are sufficient in terms of power and torque. The 10-pole models stand out for power and efficiency, but they have a larger volume than the 8-pole model (the outer diameter of the stator/rotor (8-10 poles) is given in Table 2 as 210 mm and 242 mm respectively). It can be said that the advantage of the 8-pole models is the low volume.

4. RESULTS AND EVALUATION

AF double air gap free magnet and magnet-assisted SynRM design models and analysis results are compared. Comparisons are made for these motors operating under different conditions, such as special EV, and their advantages and disadvantages are stated.

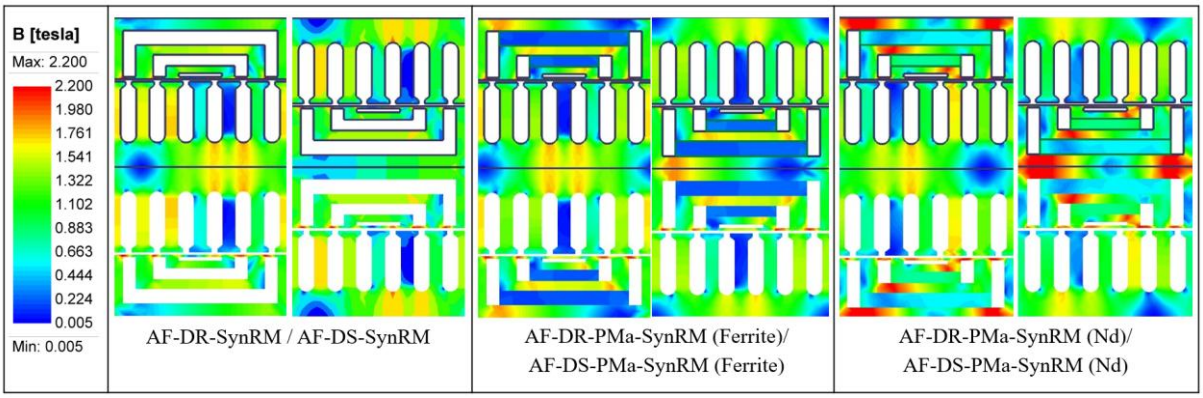

Figure 4. Flux Density Distribution of AF Double Air Gap SynRM and Magnet-Assisted SynRM Models

Figure 4 shows the flux distribution plots of the 8-pole, $J = 10 A/mm^2$ models of the AF-SynRM design study. These results were obtained by including the magnetic state in the double air gap structure of the 6, 8 and 10 pole motor models. Since the magnet-free, ferrite-assisted and RE-assisted models show similar differences at different pole numbers, only the 8-pole analysis results are shown in Figure 4.

Figure 4 shows that the flux density on the tangential rib between the barriers and the air gap gives a value of approximately 2.2 T for each model. In both the DR and DS models of AF-PMa-SynRM (RE-assisted) the flux density at the rotor yoke is higher than in the other models as expected. Because magnets have an increasing effect for magnetic flux density. In addition, unlike the other models, the flux density increases in the core/segments between the barriers of the AF-PMa-SynRM (RE-assisted) model. The flux densities observed in the DS and DR designs of the magnet-free AF-SynRM and magnet-assisted AF-PMa-SynRM (ferrite-assisted) models are mostly below 1.5 T. Only in the tangential rip section, as expected, results of about 2.2 T and above were obtained.

Magnet-free and magnet-assisted (ferrite and RE) designs of AF-SynRM models in double air gap structure are compared. Torque, power, and efficiency results of 6, 8, 10 pole motor models with double air gap (DS / DR) and magnet state (magnet-free / ferrite-assisted / RE-assisted) at the same current density ($J = 10 A/mm^2$) were analyzed.

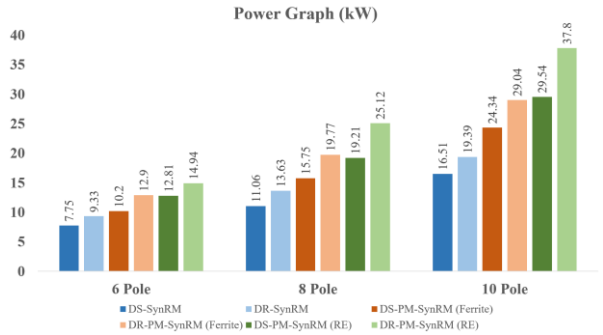

Figure 5. Comparison of Power Analysis Results of AF-SynRM Design Models

In Figure 5, when only DS and DR topologies of all models are compared, there is a maximum difference of 30% in the performance results (for DS-SynRM/DR-SynRM 8-pole models with RE-assisted). This variation between other DS and DR models is calculated to be around 17%-30%. Compared to the average power of 6-pole AF-SynRM models (DR and DS), the 8-pole design achieves 45% higher power results, and the 10-pole model achieves 110% higher power results. When a ferrite magnet is added to this model, compared to the 6-pole model; the 10-pole model has a high power value of 132% and the 8 pole model has a high power value of 54%. Looking at the average power of the 6-pole AF-SynRM models (DR and DS) with RE magnet, the 8-pole and 10-pole models achieve 72% and 161% higher power values respectively. It is clear that increasing the number of poles gives better results for all models.

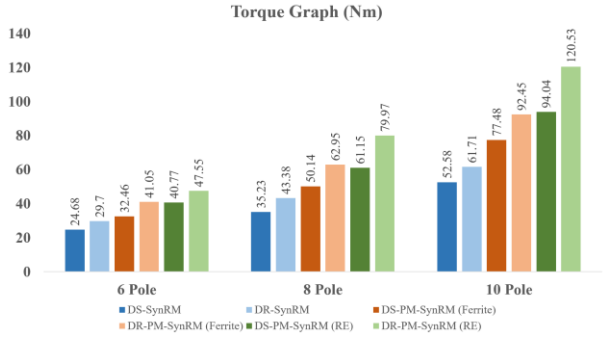

Figure 6. Comparison of Torque Analysis Results of AF-SynRM Design Models

Figure 6 shows the torque results obtained from the analysis of the DR/DS-AF-SynRM models (6-8-10 poles). For these models, the torque and power values have changed in direct proportion to the analyses for 3000 rpm constant speed. Figures 6 show an increase of 35% for the ferrite-assisted design and 51% for the RE-assisted design compared to the average torque of 6-pole magnet-free AF-SynRM motor models (DR and DS). Similarly, compared to the average torque of 8-pole magnet-free AF-SynRM motor models (DR and DS), an increase of 44% is observed in the ferrite-assisted design and 80% in the RE-assisted design. In the 10-pole magnet-free AF-SynRM motor model performance (average of DR and DS), an increase of 49% is obtained for the ferrite-assisted design and 88% for the RE-assisted design. As expected, the RE magnet-assist gives better results in each model.

The performance comparison of the AF-SynRM models designed for EV is shown in Figure 5 and Figure 6. According to the results of the analyses, the desired power value of 30 kW at the same current density was achieved in just AF-DR-SynRM RE magnet-assist models. With AF-DR-SynRM ferrite magnet-assist and RE magnet-assist AF-DS-SynRM, favorable results were obtained for 10-pole. Considering the cost and the dependency on RE-magnets, the use of ferrite magnets becomes advantageous especially for the 10-pole model. In order to achieve this power (>30 kW) with free magnet models, it is necessary to redesign at higher currents (considering the current density) or higher volumes.

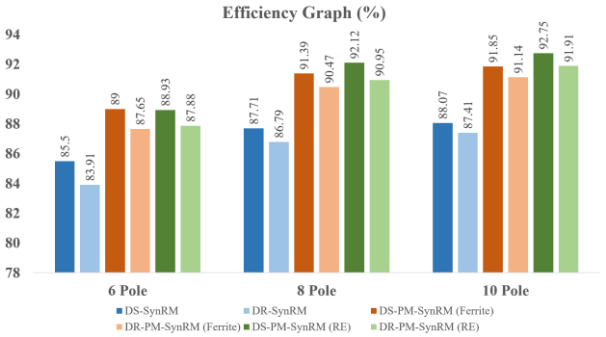

Figure 7. Comparison of Efficiency Analysis Results of AF-SynRM Design Models

As a result of the analyses, the efficiency comparison of the AF-SynRM models is shown in Figure 7. The DS topology gives slightly better results than the DR topology as the number of poles increases. It is also observed that increasing the number of poles gives positive results for all models. In Figure 7, RE-assisted models are 1%, 6% and 1% more efficient than ferrite-assisted models for 6-8-10 poles respectively. In consideration of the disadvantages of RE-magnet, it is a value that can be ignored.

The torque, power and efficiency results of the models used in this study are shown in Figure 5 to Figure 7. Analyzing these graphs, the 10-pole motor gives better results than the other motor models for each performance value. The analyses used to determine the initial design criteria were conducted with 2D linear models. Although 3D FEM analyses are necessary to increase accuracy, it is critical to perform these analyses only on the optimal model to ensure the efficient use of design time and computational resources. For EV motor design, 6-pole motor performance is insufficient. In this case it is difficult to favour it over other models. The 8-pole magnet-free motor model failed to satisfy the required performance. However, for the AF-DR-SynRM RE magnet-assisted model, results close to adequate

performance were obtained. The 8-pole models also have a weight advantage over their 6-pole and 10-pole competitors. 6-pole and 10-pole models have 1.7% and 15% more volume respectively than 8-pole models. When evaluated in terms of torque/power density, the 8-pole magnet-free model produces 45% less torque/power than the 10-pole magnet-free model at 10A/mm^2 current density. In this case, it significantly reduces its disadvantage in terms of torque/power density.

5. CONCLUSION

Due to the development of technology and the change in people's priorities, EVs have found a place in the market and are expected to increase in popularity in the future. In this case, the research to be carried out for EV is focused on the battery and the electric motor. Due to the inadequacy of battery technology, electric motors become critical in terms of vehicle efficiency and range.
According to 30 kW rated power, the SynRM design was found to be suitable as it has no winding in the rotor and magnet-free. SynRM is designed according to the double air gap AF motor topology with low volume, high power, and torque values. Due to the high number of meshes and the analysis time, a 2D linear model was used in the initial design instead of a 3D model, which gives satisfactory results in a short time. Using a 2D linear model to compare AF-SynRM models with a double air gap configuration is considered a fast and reliable method for determining the performance limits of AF-SynRM compared to 3D models with high mesh density.
The AF-SynRM model was analyzed separately for DS and DR topologies with different numbers of poles (6-8-10) and the results were compared. Considering that the motor analyses will operate at high currents and include additional cooling, the current density is limited between 10-30 A/mm^2. Magnet-free AF-SynRM achieves values of 19.39 kW power and 87.41% efficiency only with 10-pole at 10 A/mm^2 current density. Ferrite-assisted AF-DR-SynRM models achieve values of 12.9 kW, 19.77 kW and 29.04 kW for 6-8-10 poles.
According to the analysis results of the AF-SynRM models, the increase in the number of poles and the additional magnet assistance leads to an increase in performance values. Although 10-pole RE magnet assisted DR-AF-SynRM models produce 120.53 Nm torque, 91.91% efficiency and 37.8 kW power. The 10-pole DR-AF-SynRM model has been calculated to have 15% more volume than the 8-pole DR-AF-SynRM model; conversely, the 10-pole model has been shown to produce 51% more power than the 8-pole model. Additionally, the 10-pole DS-AF-SynRM model had the highest efficiency value, which was calculated as 92.75%. A design close to the nominal power was created, delivering 29.54 kW at a high efficiency level.
As a result, the study analyses the process from the initial stage to the development stage of a motor design for EV step by step. The design of the motor according to the rated power 30 kW, the effect of structural changes in the motor design on the performance are examined in a wide range. This study investigated the effects of air gap topology, pole number, and magnet assistance on the performance of the AF-SynRM model within the scope of the initial design. The necessary analyses for different current densities were performed using the 2D linear FEM on eighteen different model configurations. The 2D linear modeling approach, which is commonly used in literature for single-sided axial flux models, was also employed for double-sided models in this study, significantly reducing the computational load. This study lays the groundwork for future 3D analysis and optimization studies based on the optimal model for EVs.

DECLARATION OF ETHICAL STANDARDS

The authors of this article declare that the materials and methods used in their studies do not require ethical committee approval and/or legal-specific permission.

AUTHORS' CONTRIBUTIONS

Emre GÖZÜAÇIK: Conducted the modelling and analysis, interpreted the results, and drafted the manuscript.

Mehmet AKAR: Developed the research concept, contributed to the evaluation of the results, and reviewed and approved the final version of the manuscript.

CONFLICT OF INTEREST

There is no conflict of interest in this study.

REFERENCES

[1] M. Ehsani, K. V. Singh, H. O. Bansal, and R. T. Mehrjardi, "State of the Art and Trends in Electric and Hybrid Electric Vehicles," ***Proc. IEEE***, 109(6):967–984, (2021).

[2] A. Bozkurt, A. F. Baba, and Y. Oner, "Design of Outer-Rotor Permanent-Magnet-Assisted Synchronous Reluctance Motor for Electric Vehicles," ***Energies***, vol. 14, no. 13, p. 3739, (2021).

[3] T. Zou et al., "Airgap Length Analysis of a 350 kw PM-Assisted Syn-Rel Machine for Heavy Duty EV Traction," ***IEEE Trans. on Ind. Applicat.***, vol. 59, no. 2, pp. 1557–1570, (2023).

[4] S. Madichetty, S. Mishra, and M. Basu, "New trends in electric motors and selection for electric vehicle propulsion systems," ***IET Electrical Systems in Transportation***, vol. 11, no. 3, pp. 186–199, (2021).

[5] E. Bekiroglu and S. Esmer, "Design and Double-Stage Optimization of Synchronous Reluctance Motor for Electric Vehicles," ***Electric Power Components and Systems***, vol. 51, no. 20, pp. 2557–2572, (2023).

[6] L. Shao, D. Tavernini, A. E. Hartavi Karci, and A. Sorniotti, "Design and optimisation of energy-efficient PM-assisted synchronous reluctance machines for electric vehicles," ***IET Electric Power Appl***, vol. 17, no. 6, pp. 788–801, (2023).

[7] S. N. Jani and J. G. Jamnani, "A comparative study of electric motor for low-power density electric vehicles," ***Environ Sci Pollut Res***, (2023).

[8] M. Eker, B. Zöhra, and M. Akar, "Experimental performance verification of radial and axial flux line start permanent magnet synchronous motors," ***Electr Eng***, vol. 106, no. 2, pp. 1693–1704, (2024).

[9] Z. Cao, A. Mahmoudi, S. Kahourzade, W. L. Soong, and J. R. Summers, "A Comparative Study of Axial-Flux versus Radial-Flux Induction Machines," *in* ***2020 IEEE International Conference on Power Electronics, Drives and Energy Systems (PEDES)***, Jaipur, India: IEEE, (2020).

[10] A. Mahmoudi, S. Kahourzade, E. Roshandel, and W. L. Soong, "Axial-Flux Synchronous Reluctance Motors: Introduction of a New Machine," *in* ***2020 IEEE International Conference on Power Electronics, Drives and Energy Systems (PEDES)***, Jaipur, India: IEEE, (2020).

[11] F. Nishanth, J. Van Verdeghem, and E. L. Severson, "A Review of Axial Flux Permanent Magnet Machine Technology," ***IEEE Trans. on Ind. Applicat.***, vol. 59, no. 4, pp. 3920–3933, (2023).

[12] F. Farrokh, A. Vahedi, H. Torkaman, and M. Banejad, "Design and comparison of dual-stator axial-field flux-switching permanent magnet motors for electric vehicle application," ***IET Electrical Syst in Trans***, vol. 13, no. 2, p. e12074, (2023).

[13] L. Shao, A. E. H. Karci, D. Tavernini, A. Sorniotti, and M. Cheng, "Design Approaches and Control Strategies for Energy-Efficient Electric Machines for Electric Vehicles—A Review," ***IEEE Access***, vol. 8, pp. 116900–116913, (2020).

[14] F. Un-Noor, S. Padmanaban, L. Mihet-Popa, M. Mollah, and E. Hossain, "A Comprehensive Study of Key Electric Vehicle (EV) Components, Technologies, Challenges, Impacts, and Future Direction of Development," ***Energies***, vol. 10, no. 8, p. 1217, (2017).

[15] K. Deepak, M. A. Frikha, Y. Benômar, M. El Baghdadi, and O. Hegazy, "In-Wheel Motor Drive Systems for Electric Vehicles: State of the Art, Challenges, and Future Trends," ***Energies***, vol. 16, no. 7, p. 3121, (2023).

[16] A. Limane Mahamat, E. Gözüaçık, and M. Akar, "Sensitivity-Based Design and Optimization of Line Start Synchronous Reluctance Motor," ***Electric Power Components and Systems***, 51(20):2499–2511, (2023).

[17] M. Al-ani, A. Walker, G. Vakil, D. Gerada, C. Gerada, and K. Paciura, "Modifications to PM-Assisted Synchronous Reluctance Machine to Achieve Rare-Earth Free Heavy-Duty Traction," ***IEEE J. Emerg. Sel. Topics Power Electron.***, 11(2):2029–2038, (2023).

[18] E. Eser and N. Üstkoyuncu, "Effects of Permanent Magnets on Different Flux Barriers for the AF-SynRMs," ***Electric Power Components and Systems***, 52(10):1936–1945, (2024).

[19] M. Soyaslan, Y. Avşar, A. FenerciOglu, and F. Sarihan, "Design and Production of Belt Drive Elevator Traction Machine: Modelling of Double Side Belt System," ***Journal of Polytechnic***, (2023).

[20] P. Ragazzo, S. Ferrari, G. Dilevrano, L. Beatrici, C. Girardi, and G. Pellegrino, "Scaling of Ferrite-assisted Synchronous Reluctance Machines for Lifting Systems," *in 2023* ***IEEE Workshop on Electrical Machines Design, Control and Diagnosis (WEMDCD)***, Newcastle upon Tyne, United Kingdom: IEEE, (2023).

[21] G. Du, G. Zhang, H. Li, and C. Hu, "Comprehensive Comparative Study on Permanent-Magnet-Assisted Synchronous Reluctance Motors and Other Types of Motor," ***Applied Sciences***, vol. 13, no. 14, p. 8557, (2023).

[22] V. Dmitrievskii, V. Kazakbaev, and V. Prakht, "Performance Comparison of Traction Synchronous Motors with Ferrite Magnets for a Subway Train: Reluctance versus Homopolar Variants," ***Applied Sciences***, vol. 13, no. 17, p. 9988, (2023).

[23] H. S. Gercekcioglu and M. Akar, "Optimal rotor design of novel axial flux synchronous reluctance motor and validation," ***Int Trans Electr Energ Syst***, vol. 31, no. 5, (2021).

[24] M. Özsoy, O. Kaplan, and M. Akar, "The effect of stator slot number and pole number on motor performance in double-sided axial flux induction motors for electric vehicles," ***Electr Eng***, vol. 104, no. 6, pp. 4289–4304, (2022).

[25] E. Gözüaçık and M. Akar, "Senkron Relüktans Motor Analitik Hesabı ve Tasarımı," ***Gaziosmanpasa Journal of Scientific Research (GBAD)***, vol. 12, no. 1, pp. 86–100, (2023).

[26] H. Apaydın, F. Serteller, and Y. Oğuz, "Implementation of Three Phase Induction Motor Pre-Design Program on Electronic Circuit," ***Journal of Polytechnic***, vol. 27, no. 4, pp. 1281–1292, (2024).

[27] H. Aghazadeh, E. Afjei, and A. Siadatan, "Sizing and detailed design procedure of external rotor synchronous reluctance machine," ***IET Electric Power Applications***, vol. 13, no. 8, pp. 1105–1113, (2019).

[28] O. Mısır and M. Akar, "Efficiency and Core Loss Map Estimation with Machine Learning Based Multivariate Polynomial Regression Model," ***Mathematics***, vol. 10, no. 19, p. 3691, (2022).

[29] E. Roshandel, A. Mahmoudi, S. Kahourzade, A. Yazdani, and G. Shafiullah, "Losses in Efficiency Maps of Electric Vehicles: An Overview," ***Energies***, 14(22):7805, (2021).

[30] H. S. GerçekciOğlu and M. Akar, "Efficiency and Performance Comparison Between Synchronous Reluctance and Induction Motor in Axial Flux Concept," ***Gazi University Journal of Science PART C: Design and Technology***, 9(2):297–316, (2021).

[31] A. Nyitrai and M. Kuczmann, "Magnetic equivalent circuit and finite element modelling of anisotropic rotor axial flux permanent magnet synchronous motors with fractional slot distributed winding," ***IET Electric Power Appl***, vol. 17, no. 5, pp. 709–720, (2023).

[32] J. Wang, Z. Xu, Z. Xing, Y. Liu, and W. Ji, "Study on Electromagnetic Performance of Skewed Permanent Magnet Axial Flux Permanent Magnet Synchronous Motor," J. ***Electr. Eng. Technol.***, (2024).

[33] E. Gözüaçık, "Elektrikli Araç Uygulamaları için Eksenel Akılı Sabit Mıknatıs Destekli Senkron Relüktans Motor Tasarımı ve Analizi," Doctoral Thesis, Tokat Gaziosmanpaşa University, Tokat, (2025).

[34] A. Walker, M. Galea, D. Gerada, C. Gerada, A. Mebarki, and N. Brown, "Development and design of a high performance traction machine for the FreedomCar 2020

traction machine targets," *in 2016* ***XXII International Conference on Electrical Machines (ICEM)***, Lausanne, Switzerland: IEEE, pp. 1611–1617, (2016).

[35] M. Özsoy, O. Kaplan, and M. Akar, "Implementation of Different 2D Finite Element Modeling Approaches in Axial Flux Induction Motors," ***Electric Power Components and Systems***, vol. 51, no. 19, pp. 2385–2396, (2023).

[36] A. M. Ajamloo, M. N. Ibrahim, and P. Sergeant, "Design, Modelling and Optimization of a High Power Density Axial Flux SRM with Reduced Torque Ripple for Electric Vehicles," ***Machines***, vol. 11, no. 7, p. 759, (2023).

[37] M. Gulec and M. Aydin, "Implementation of different 2D finite element modelling approaches in axial flux permanent magnet disc machines," ***IET Electric Power Appl***, vol. 12, no. 2, pp. 195–202, (2018).

[38] E. Gözüaçık, M. Eker, and M. Akar, "Multislice Analysis of Axial Flux Synchronous Reluctance Motor Based on 2d Finite Element Method Linear Model," ***JMAG***, vol. 28, no. 2, pp. 219–226, (2023).

[39] A. Akay, "Driving a Symmetric Permanent Magnet Synchronous Six-Phase Machine with Consecutive Three Phases," ***Journal of Polytechnic***, vol. 27, no. 6, pp. 2139–2149, (2024).

[40] E. Gözüaçık and M. Akar, "Multi-Physics and Multi-Objective Design of an Axial Flux Permanent Magnet-Assisted Synchronous Reluctance Motor for Use in Electric Vehicles," ***Machines***, vol. 13, no. 7, Art. no. 7, (2025).

[41] Y. Gai et al., "Cooling of Automotive Traction Motors: Schemes, Examples, and Computation Methods," ***IEEE Trans. Ind. Electron.***, vol. 66, no. 3, pp. 1681–1692, (2019).